INSTITUTE OF PHYSICS PUBLISHING and INTERNATIONAL ATOMIC ENERGY AGENCY NUCLEAR FUSION

Nucl. Fusion **46** (2006) S275–S280 doi:10.1088/0029-5515/46/6/S07

Modelling of negative ion transport in caesium-seeded volume negative ion sources

Osamu Fukumasa and Ryo Nishida

Department of Electrical and Electronic Engineering, Faculty of Engineering, Yamaguchi University, Tokiwadai 2-16-1, Ube 755-8611, Japan

Received 4 July 2005, accepted for publication 25 October 2005
Published 22 May 2006
Online at stacks.iop.org/NF/46/S275

Abstract

Trajectories of H^- ions are calculated numerically by solving the 3D motion equation, including effects of collisional destruction, elastic collisions and charge exchange collisions. According to these trajectories, the extraction probability of H^- ions produced at any location inside the source and the energy relaxation of extracted H^- ions are estimated as a function of gas pressure. Effects of production zone and field intensity of the magnetic filter on extraction probability are also discussed. The extraction probability of surface produced H^- ions is much higher than that of volume produced H^- ions. The kinetic energy of extracted H^- ions is reduced mainly by charge exchange collisions with H in higher pressure region and by elastic collisions with H^+ in lower pressure region.

We also briefly discuss the pressure dependence of extracted negative ion currents combining the present numerical results and the results of the model calculation with the zero-dimensional code.

PACS numbers: 29.25.Ni, 52.65.Cc, 52.65.Pp

1. Introduction

Negative ion based neutral beam injection is one of the most promising candidates for heating and current drive of fusion plasma. By seeding a small amount of caesium (Cs) vapour into the volume ion source, H^- production increases by a factor of 2–4 and optimum pressure decreases to 0.8–1.0 Pa [1]. Although Cs effects have been observed by many researchers, the mechanism remains to be discussed. We have studied source modelling [2–6] and Cs effects on the enhancement of H^- production in a tandem two-chamber system, i.e. the source and the extraction regions. According to our numerical results, it is confirmed that the dominant process for the enhancement of H^- production is surface production [5, 6].

For discussing the pressure dependence of extracted H^- current, we have also estimated the extracted H^- ions, by taking into account only stripping loss in the acceleration grid region [4, 5]. But, many H^- ions produced in the source could not be extracted because of collisional destructions. So, it is important to study the behaviour of H^- ions in the second chamber, i.e. in the production and extraction regions [7]. In addition, it has been reported that the beam divergence of surface produced H^- ions are nearly the same as that of volume produced H^- ions [8]. However, the physical reason has not yet been clarified.

In this paper, we will discuss the pressure dependence of the extraction probability of H^- ions using both the model calculation [5] and H^- ion transport in the second chamber [7]. The preliminary results have been presented earlier [9, 10]; herewith H^- ion transport and extracted H^- ions are further studied including the effects of production zone and intensity of the magnetic filter (MF). To clarify good beam optics of surface produced H^- ions, we will also estimate both mean kinetic energy (KE) and the velocity distribution of extracted H^- ions.

2. Simulation model and procedure

To simulate H^- production in a tandem two-chamber system, we have used the zero-dimensional code with the source model, shown in figure 1 [3–5]. In the present study, using a coordinate system shown in figures 1 and 2, negative ion trajectory in the second chamber is calculated numerically, with width L = 30 cm. The MF is set at 2 cm ($=L_2$) upstream from a plasma grid (PG). Spatial profile of the field intensity for the MF is given by the Gaussian profile $B_x(z) = B_0 \exp[-(z-z_0)^2/l_B^2]$, where z_0 = 2 cm, l_B = 4 cm and B_0 = 120 G. Surface confinement magnetic field, i.e. the line cusp magnetic field, is also present. Sixteen columns of permanent magnets are arranged to construct the line cusp magnetic field.

When a negative ion is produced, it moves inside the source until destruction or extraction. Trajectories of H^- ions are calculated numerically by solving the three-dimensional

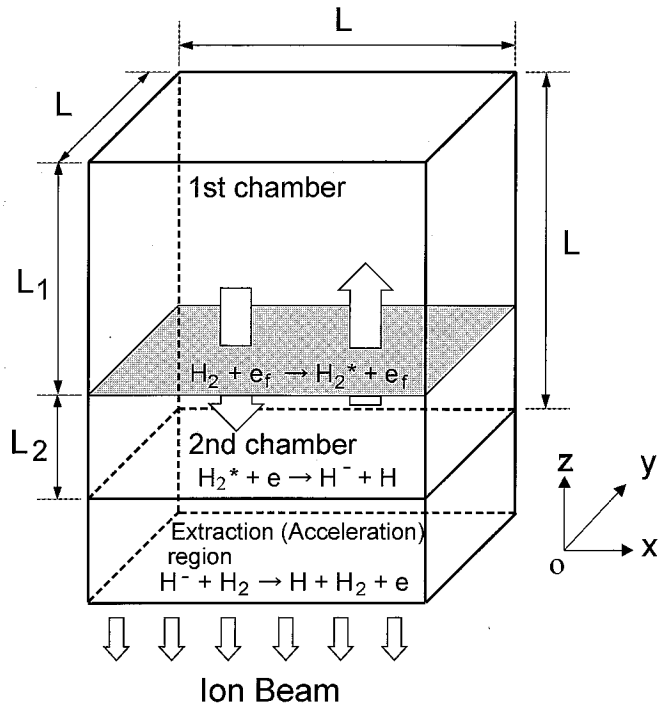

Figure 1. Simulation model for the tandem two-chamber system.

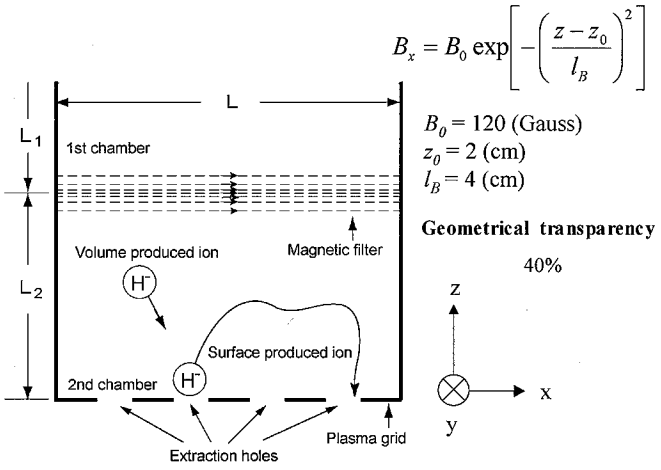

Figure 2. Model geometry of the second chamber used for the tandem system shown in figure 1.

motion equation as follows:

$$\frac{M\,\mathrm{d}\boldsymbol{v}}{\mathrm{d}t} = q(\boldsymbol{v}\times\boldsymbol{B}) + \boldsymbol{F}_{\mathrm{col}}, \tag{1}$$

where M is the mass of the H^- ion, q is the charge, $\boldsymbol{v}$ is the velocity vector and $\boldsymbol{B}$ the vector of magnetic field. The electric field is neglected in the above equation because it is negligibly small in the plasma region as compared with the electric field in the sheaths near the PG and chamber walls. The second term on the right-hand side, $\boldsymbol{F}_{\mathrm{col}}$, is the collision term, which is explained below. When $\boldsymbol{x}$ is the vector of the position, the definition of velocity vector can be described as

$$\frac{\mathrm{d}\boldsymbol{x}}{\mathrm{d}t} = \boldsymbol{v}. \tag{2}$$

We solved equations (1) and (2) in three dimensions using the Runge–Kutta–Gill method as the initial value problem.

The collisional effects between H^- ions and other particles are calculated by the Monte Carlo method [7, 11]. The following destructions, charge exchange and elastic collisions, are taken into account:

$H^- + e \rightarrow H + 2e$	electronic detachment (ED)	(3)
$H^- + H^+ \rightarrow 2H$	mutual neutralization (MN)	(4)
$H^- + H_2^+ \rightarrow H + H_2$		(5)
$H^- + H_3^+ \rightarrow 2H + H_2$		(6)
$H^- + H \rightarrow H_2 + e$	associative detachment (AD)	(7)
$H^- + H_2 \rightarrow H + H_2 + e$		(8)
$H^- + Cs^+ \rightarrow H + Cs$		(9)
$H^- + Cs \rightarrow H + Cs + e$		(10)
$H^- + H \rightarrow H + H^-$	charge exchange (CX) with H atoms [12]	(11)
$H^- + H^+ \rightarrow H^- + H^+$	elastic collision (EC) with H^+ ions	(12)

Volume produced H^- ions are launched isotropically in all directions with an initial energy of 0.5 eV at any x, y location, except that axial points (z direction), where there are four launching points (i.e. z = 0.25, 0.75, 1.25 and 1.75 cm), were used. The surface produced H^- ions are launched from the PG with an initial energy of 0.5, 1 and 2 eV due to potential difference between the plasma potential and the PG potential. When H^- ions have reached the PG or destroyed by collisional processes, the calculation is finished.

The background plasma profiles, i.e. particle densities, are assumed to be uniform, and these values are obtained by the model calculation [4, 5] and used to estimate mean free paths of H^- ions for the collisions mentioned above. For example, to determine the electron density dependence of H^- production and particle densities, calculation is performed as a function of electron density $n_e(1)$ in the first chamber on the assumption that other plasma parameters are kept constant [3–5]. A typical numerical result of the model calculation are summarized in table 1. Plasma conditions for calculation are as follows: the gas pressure p = 5 mTorr, the electron density ratio between two chambers $n_e(2)/n_e(1)$ = 0.2, density of e_f in the first chamber $n_{e_f}(1)/n_e(1)$ = 0.05, electron temperature in the first and second chambers are, respectively, $\kappa T_e(1)$ = 5 eV, $\kappa T_e(2)$ = 1 eV and MF position $L_1 : L_2$ = 28 : 2 cm (i.e. $z_0 = L_2$ = 2 cm).

3. Numerical results and discussion

3.1. Extraction probability and energy relaxation of negative ions

The trajectories of H^- ions are obtained by solving the three-dimensional motion equation until ions are destroyed or extracted (i.e. reached to the PG). For reference, typical orbits of H^- ions in the second chamber of the negative ion source are shown in figure 3.

Table 1. Some plasma parameters obtained by the model calculation when hydrogen gas pressure $p = 5$ mTorr.

n_{H^-}	H^- ion density	3.81×10^{11} cm^{-3}
n_e	Electron density	1.00×10^{12} cm^{-3}
n_H	H atom density	5.22×10^{13} cm^{-3}
n_{H_2}	H_2 atom density	8.31×10^{13} cm^{-3}
n_{H^+}	H^+ ion density	3.73×10^{11} cm^{-3}
$n_{H_2^+}$	H_2^+ ion density	2.71×10^{11} cm^{-3}
$n_{H_3^+}$	H_3^+ ion density	1.52×10^{11} cm^{-3}
n_{Cs^+}	Cs^+ ion density	5.85×10^{11} cm^{-3}
n_{Cs}	Cs atom density	4.41×10^{12} cm^{-3}
T_e	Electron temperature	1.0 eV
T_H	H atom temperature	0.5 eV
T_{H^+}	H^+ ion temperature	0.5 eV

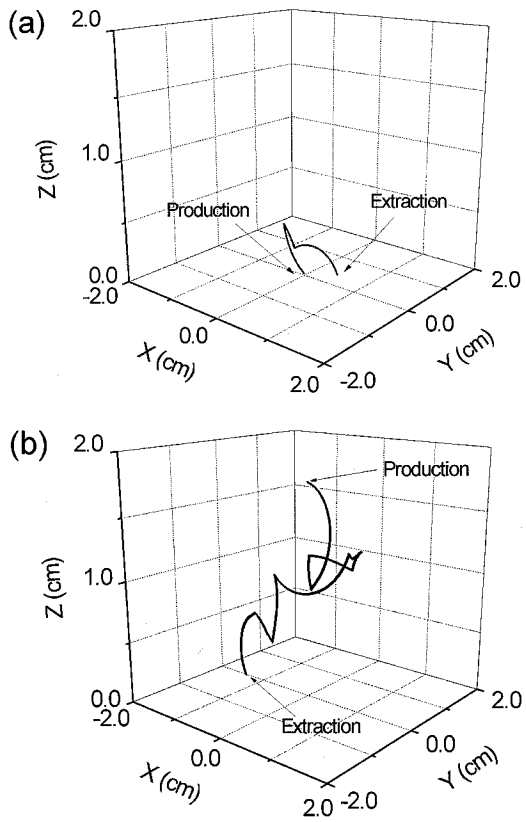

Figure 3. Examples of H^- ion trajectories in the second chamber: (*a*) a surface produced H^- ion (initial energy: 1 eV, birth point $(x, y, z) = (0, 0, 0)$) and (*b*) a volume produced H^- ion (initial energy: 0.5 eV, birth point $(x, y, z) = (0, 0, 1.75$ cm)).

At first, characteristic features of H^- ion trajectories (i.e. properties on H^- ion extraction) are discussed. To this end, a set of five calculations (one calculation for surface produced H^- ions and four calculations for volume produced H^- ions with different four z positions) is done under certain plasma conditions. We used 10^3 test H^- ions for one calculation. Table 2 shows the simulation result, where gas pressure is 5 mTorr. In the present case, 710 surface produced H^- ions reached the PG and extraction probability is about 28.4% (geometrical transparency of the PG is assumed to be 40%). For volume produced H^- ions, the probability to reach the PG depends strongly on the upstream distance z from the PG. Then, the mean value of the extraction probability is about 5.2%.

This probability depends on gas pressure. Table 3 shows another example of the simulation result, where gas pressure is 1 mTorr. According to the results in tables 2 and 3, the extraction probability of volume produced H^- ions slightly decreases with gas pressure. These characteristic features are clearly shown in figure 4. The effect of MF field on H^- trajectories is also discussed. The numerical result is shown in figure 5, where gas pressure is 5 mTorr and $B_0 = 120$ G for two different l_B, i.e. 1 and 4 cm. There is scarcely any difference in the extraction probability due to the difference in the field intensity of the MF.

H^- ion transport (i.e. the extraction probability) depends on gas pressure. Discussing this point, the same calculations described above are done by changing the gas pressure. In the present calculation, initial positions (i.e. birth points) of surface produced H^- ions are distributed at any location on the PG and those of volume produced H^- ions are also distributed at any location in the second chamber, i.e. three-dimensional. Now, 10^3 test particles for surface produced H^- ions and 2×10^3 test particles for volume produced H^- ions are used, respectively.

The numerical results are shown in figure 6. The extraction probability of volume produced H^- ions decreases with gas pressure in nearly the same manner as that of surface produced H^- ions. It is remarkable, however, that the extraction probability of surface produced H^- ions is much higher than that of the volume produced H^- ions. The physical meaning is as follows: with increasing gas pressure, particle densities increase and mean free path of H^- ions decreases in its value. Therefore, the transport of H^- ions in the extraction region decreases due to collisional effects. In particular, surface produced H^- ions injected into plasmas are reflected easily by elastic and charge exchange collisions and then reach the PG. On the other hand, volume produced H^- ions are impended to reach the PG by collisional processes.

Kinetic energy (KE) of H^- ions are reduced by elastic [13] and charge exchange [7] collisions. According to table 2, for surface produced H^- ions with initial energy 1 eV, the averaged KE of the extracted H^- ions is reduced to 0.66 eV. On the other hand, for volume produced H^- ions with 0.5 eV, the averaged KE of the extracted H^- ions is reduced to 0.45 eV, and lower than that of surface produced H^- ions due to a difference in the initial energy of H^- ions. Although there is some difference between the averaged KE of extracted H^- ions for surface produced H^- ions and that for volume produced H^- ions, energy relaxation mentioned above is the cause for good beam optics of negative ion current with Cs seeding [8]. As is shown in table 2, in the high-pressure case, charge exchange collision is the most dominant collision process. With decreasing p (see table 3), however, effects of elastic collisions become remarkable. Therefore, both elastic and charge exchange collisions play important roles in the energy relaxation of the extracted H^- ions.

In the present calculation, for estimating the extraction probability, as is mentioned in section 2, the background plasma profiles (i.e. particle densities) are assumed to be uniform. But, in a plasma-sheath region, maybe the density of charged particles should be described as functions of the positions from the PG, thereby affecting the number of recombination events. This can be an item for future studies.

Table 2. Numerical results of H^- transport, where $p = 5$ mTorr, $B_0 = 120$ G and $l_B = 4$ cm.

	H^- ions				
	Surface produced H^- ions	Volume produced H^- ions Birth point from the PG [cm]			
		0.25	0.75	1.25	1.75
Collisions					
Wall loss	16	31	51	53	57
Collisional destruction					
e	13	24	65	127	258
H^+	33	83	113	127	103
H_2^+	26	68	87	79	70
H_3^+	11	31	46	33	33
H	44	115	165	162	145
H_2	80	186	242	257	196
Cs^+	57	55	103	99	97
Cs	10	28	33	36	27
Total	274	590	854	920	929
Elastic collision, H^+	682	1494	2161	1999	1517
Charge exchange, H	1464	3007	4416	4389	3776
H^- ions reach the PG	710	379	95	27	14
Average energy of the above H^- ions [eV]	0.66	0.46	0.42	0.44	0.48
Extraction probability [%]	28.4	15.2	3.8	1.1	0.6
				Mean value	5.2%

Table 3. Numerical results of H^- transport, where $p = 1$ mTorr, $B_0 = 120$ G and $l_B = 4$ cm.

	H^- ions				
	Surface produced H^- ions	Volume produced H^- ions Birth point from the PG [cm]			
		0.25	0.75	1.25	1.75
Collisions					
Wall loss	29	54	71	77	68
e	20	59	117	185	346
H^+	36	98	130	129	118
H_2^+	20	41	54	56	55
H_3^+	1	9	11	11	6
H	13	54	64	88	80
H_2	23	63	99	83	56
Cs^+	88	161	242	230	203
Cs	10	37	49	59	43
Total	211	522	766	841	907
Elastic collision, H^+	1043	3047	3992	3992	2942
Charge exchange, H	428	1199	1678	1865	2212
H^- ions reach the PG	760	424	163	82	25
Average energy of the above H^- ions [eV]	0.69	0.46	0.42	0.44	0.49
Extraction probability [%]	30.4	17.0	6.5	3.3	1.0
				Mean value	7.0%

3.2. Estimation of extracted negative ion currents

Next, we will discuss the pressure dependence of the extracted H^- current. Figure 7 shows the H^- densities in the second chamber, H^- (2), obtained by the model calculation [3–5] as a function of p for $n_e(1) = 5 \times 10^{12}$ cm^{-3}. In this calculation, surface productions of H^- ions and $H_2(v'')$ from H and positive ions are included. Details on wall conditions are reported elsewhere [5]. For the no Cs case, H^- ions are produced by the so-called two-step pure volume process. With Cs, however, H^- (2) increases markedly due to surface production of H^- ions from H and positive ions [4, 5].

In order to discuss the pressure dependence of the extracted H^- current [4, 5], previously, we estimated the extracted H^- ions from H^- (2) by taking into account only stripping loss of H^- ions in the extraction and acceleration grids region (see figure 1). According to gas pressure distribution along the beam axis estimated by the Monte Carlo simulation [14], we calculate the survival factor F against the stripping loss of H^- ions, i.e. $H^- + H_2 \rightarrow H + H_2 + e$ and $H^- + H \rightarrow 2H + e$. F is a decreasing function of pressure. Then, the extracted H^- ions, corresponding to the results in figure 7, are estimated by the product of H^-(2) in figure 7 with F. Namely, it is assumed that all H^- ions in the second chamber are extracted.

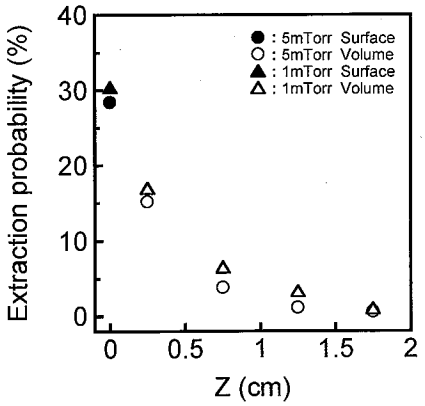

Figure 4. Extraction probability as a function of z. Parameter is hydrogen gas pressure, where $B_0 = 120$ G and $l_B = 4$ cm.

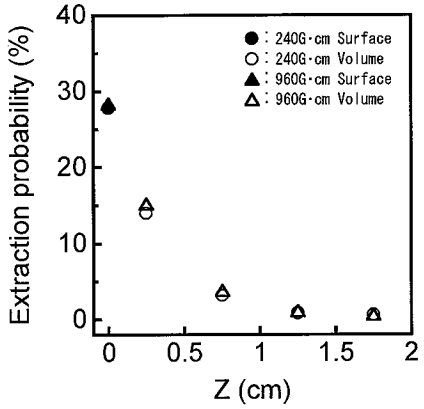

Figure 5. Extraction probability as a function of z. Parameter is MF field, where gas pressure $p = 5$ mTorr.

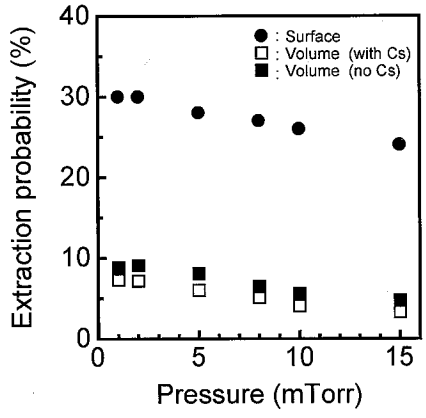

Figure 6. Pressure dependence of extraction probability for H^- ions: (●) for surface produced H^- ions, (□) and (■) for volume produced H^- ions with Cs and no Cs.

As is discussed in section 3.1, only a part of H^- ions in the second chamber can be extracted. So, the previous values of extracted H^- ions are overestimated.

Now, we will discuss and estimate the extracted H^- ions more precisely, applying the results in section 3.1, from the results in figure 7. The procedure is as follows: at first, H^- (2) density is divided into two parts, i.e. surface produced H^- ions and volume produced H^- ions, using the rates of surface production and volume production in the rate equation for H^- (2). Next, according to the extraction probabilities for

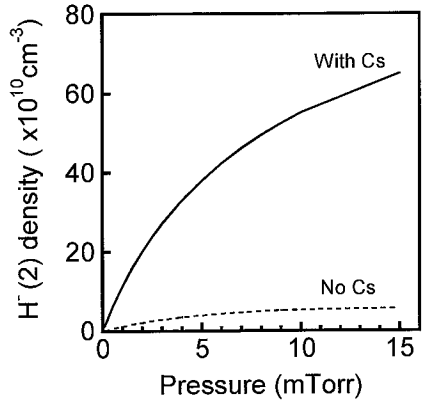

Figure 7. Pressure dependence of hydrogen negative ions obtained by model calculation: H^- (2) versus gas pressure p with Cs and no Cs, where $T_e(1) = 5$ eV, $T_e(2) = 1$ eV and $n_e(1) = 5 \times 10^{12}$ cm^{-3}.

both surface and volume produced H^- ions, H^- ions which can reach the PG are estimated from the product of H^- ion densities of two types with the extraction probabilities, respectively. Then, total H^- ions are obtained by summing up those two parts. Finally, the extracted H^- ions are determined by the product of the above-mentioned total H^- ions with survival factor F. This procedure is summarized in table 4.

Figure 8 shows the extracted H^- ions with Cs, corresponding to the result in figure 7, as a function of p. The solid line is the previous result [4, 5] and solid points are the present estimated values. The values obtained presently are much lower than the previous ones. This discrepancy is caused by the difference in the extraction probability of negative ions between the present calculation and the previous one. In the previous estimation, we assumed that all H^- ions in the second chamber could reach the PG. Namely, the extraction probability is assumed to be 100%. By taking into account collisional destruction of H^- ions, however, it is confirmed that the extraction probability of H^- ions should be reduced to be lower than 30% for surface-produced H^- ions and to be lower than 10% for volume-produced H^- ions, respectively (see table 4).

The same calculation described above is also applied to pure volume produced H^- ions (no Cs) in figure 7. Then, a new estimation of the extracted H^- ions with Cs and no Cs is shown in figure 9. In both cases, the optimum pressure giving the highest H^- currents is observed clearly. With Cs injection, the extracted H^- current increases by many times compared with the current in pure volume case.

So far, we present only one example concerning the extraction of H^- current. To discuss the pressure dependence of the extracted H^- current, more numerical results for different $n_e(1)$ should be required [5]. At any rate, the extraction probability depends strongly on the upstream distance from the PG (i.e. the extraction grid). Then, to increase the extracted negative ion currents, production of negative ions near the extraction grid should be enhanced much more.

4. Conclusions

The extraction probability for H^- ions, i.e. to reach the PG (i.e. extraction probability), is estimated. It is confirmed that

Table 4. Procedure for the estimation of extracted H^- ions, corresponding to the result shown in figure 7.

		Pressure [mTorr]					
		1	2	5	8	10	15
H^- ion density in the 2nd chamber [$\times 10^{10}$ cm^{-3}]		11.4	20.2	38.1	49.5	55.1	65.0
A rate of H^- formation [%]	SP	73.6	73.4	74.1	74.9	75.5	76.9
	VP	26.4	26.6	25.9	25.1	24.5	23.1
Estimated H^- ions [$\times 10^{10}$ cm^{-3}]	SP	8.39	14.8	28.2	37.1	41.6	50.0
	VP	3.01	5.36	9.87	12.4	13.5	15.0
Extraction probability of H^- ions [%]	SP	30	30	28	27	26	24
	VP	7.3	7.2	6.0	5.1	4.1	3.3
H^- ions reach the PG [$\times 10^{10}$ cm^{-2}]	SP	2.55	4.39	8.01	10.0	10.9	12.2
	VP	0.22	0.38	0.59	0.63	0.55	0.49
H^- ions reach the PG (total) [$\times 10^{10}$ cm^{-2}]		2.77	4.77	8.60	10.6	11.5	12.7
Survival factor F against the stripping loss [%]		94.2	88.8	74.3	62.2	55.2	40.9
Extract H^- density from the ion source [$\times 10^{10}$ cm^{-3}]		2.61	4.24	6.39	6.62	6.36	5.19

Note: SP: surface production, VP: volume production.

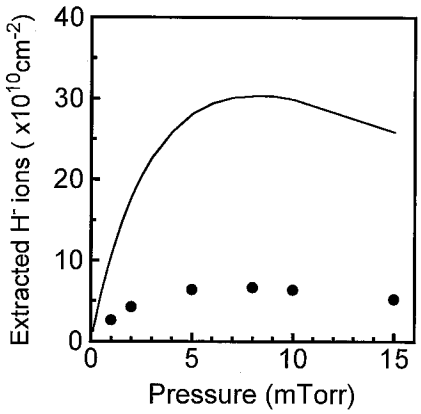

Figure 8. Estimation of the extracted H^- ions with Cs: extracted H^- ions versus p, corresponding to the results shown in figure 7, where the solid line shows the previous result and the dotted circle shows the present results.

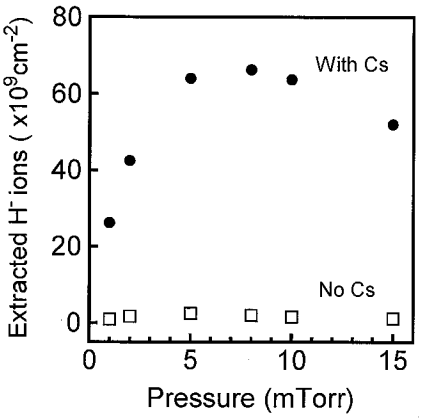

Figure 9. Extracted H^- ions versus p, corresponding to the results shown in figure 7.

the extraction probability for surface produced H^- ions is much higher than that for volume produced H^- ions. As a whole, the extraction probability is relatively low. Within the present numerical conditions, the extraction probability for surface produced H^- ions keeps a relatively high value (i.e. 24–30%) and that for volume produced H^- ions decreases in its value from 8% to 3% with increasing gas pressure. The KE of the extracted H^- ions is also reduced by both charge exchange collisions with H and elastic collisions with H^+. There is a certain energy difference in extracted H^- ions between the energy of the volume produced H^- ions and that of the surface produced H^- ions. We have also discussed briefly the characteristics of extracted negative ion current with the use of both the present numerical results for the extraction probability and the results of our previous model calculation.

Acknowledgments

The authors would like to thank Professor H. Naitou and S. Mori for their discussion and support in the preparation of the present paper. A part of this work was supported by the Grant-in-Aid for Scientific Research from the Ministry of Education, Culture, Sports, Science and Technology, Japan. This work was also performed with the support of the NIFS LHD Project Research Collaboration.

References

[1] Okumura Y. *et al* 1992 *Rev. Sci. Instrum.* **63** 2708
[2] Fukumasa O. 1989 *J. Phys. D: Appl. Phys.* **22** 1668
[3] Fukumasa O. 1992 *J. Appl. Phys.* **71** (1992) 3193
[4] Fukumasa O. and Monji H. 2000 *Rev. Sci. Instrum.* **71** 1234
[5] Fukumasa O. 2000 *IEEE Trans. Plasma Sci.* **28** 1009
[6] Fujioka T., Fukuchi T. and Fukumasa O. 2001 *Proc. 25th Int. Conf. on Phenomena in Ionized Gases (Nagoya, Japan)* vol 2 p 245
[7] Riz D. and Pamela J. 1998 *Rev. Sci. Instrum.* **69** 914
[8] Miyamoto K. *et al* 1995 *Proc. 18th Symp. on Fusion Technology (Karlsruhe, Germany)* vol 1 p 625
[9] Fukumasa O., Fukuchi T. and Fujioka T. 2002 *Proc. 9th Int. Symp. on the Production and Neutralization of Negative Ions and Beams (Gif-sur-Yvette, France), AIP Conf. Proc.* vol 639 p 75
[10] Fukumasa O. and Nishida R. 2004 *Proc. 10th Int. Symp. on the Production and Neutralization of Negative Ions and Beams (Kiev, Ukraine), AIP Conf. Proc.* vol 763 p 159
[11] Ido S., Hasebe H. and Fujita Y. 1993 *Japan. J. Appl. Phys.* **32** 4761
[12] Hummer D.G., Stebbings R.F., Fite W.L. and Branscomb L.M. 1960 *Phys. Rev.* **119** 668
[13] Makino K., Sakurabayashi T., Hatayama A., Miyamoto K. and Ogasawara M. 2002 *Rev. Sci. Instrum.* **73** 1051
[14] Takeiri Y., Ando A., Kaneko O., Oka Y., Tsumori K., Akiyama R., Asano E., Kawamoto T., Kuroda T. and Kawakami H. 1995 *Rev. Sci. Instrum.* **66** 2541